RSC Advances

PAPER

View Article Online
View Journal | View Issue

Cite this: *RSC Adv.*, 2016, **6**, 41871

Multifunctional Fe_3O_4@*n*SiO_2@*m*SiO_2/Pr-Imi-$NH_2\cdot$Ag core–shell microspheres as highly efficient catalysts in the aqueous reduction of nitroarenes: improved catalytic activity and facile catalyst recovery

Mina Jafari Nasab and Ali Reza Kiasat*

Core@shell nanoparticles with a superparamagnetic iron oxide core, a middle nonporous silica shell, and an outer organo functionalized mesoporous silica shell were synthesized and evaluated for immobilizing Ag nanoparticles. The iron oxide nanoparticles cores were synthesized *via* improved chemical coprecipitation method and they were silica-coated by surface silylation *via* a Stober sol–gel process. Afterward, magnetic core–shell structured mesoporous silica microspheres, Fe_3O_4@*n*SiO_2@*m*SiO_2, were synthesized by silylation of Fe_3O_4@*n*SiO_2 surface using tetraethyl orthosilicate through surfactant directed self-assembly on the surface, followed by etching of the surfactant molecules. Further modification of the surface by grafting of 3-chloropropyl triethoxysilane, nucleophilic substitution reaction of the chloride with imidazole and then quaternization with 2-bromo ethylamine hydrobromide produced the 2-amino ethyl-3-propyl imidazolium bromide functionalized magnetic core–shell structured mesoporous silica microspheres, Fe_3O_4@*n*SiO_2@*m*SiO_2/Pr-Im-NH_2. Finally, the target nanocomposite, Fe_3O_4@*n*SiO_2@*m*SiO_2/Pr-Im-$NH_2\cdot$Ag was formed by embedding the silver nanoparticles into the mesoporous nanocomposite. The organic–inorganic nanocomposite was characterized by FT-IR spectroscopy, transmission electron microscopy (TEM), elemental analysis (CHN), vibrating sample magnetometer (VAM), thermogravimetric analysis (TGA) and differential thermal analysis (DTA), X-ray diffraction (XRD) and Brunauer–Emmett–Teller (BET). The catalytic activity test with the nitroarene reduction in an aqueous medium by using $NaBH_4$ reveals that this Ag-supported nanocomposite is highly active for a wide range of substrates, suggesting highly promising application potentials of the magnetic core–shell-structured mesoporous organosilica. This method has the advantages of high yields, a cleaner reaction, simple methodology, short reaction times, easy workup, and greener conditions. In addition to the facility of this methodology, it also enhances product purity and promises economic as well as environmental benefits.

Received 3rd January 2016
Accepted 2nd March 2016

DOI: 10.1039/c6ra00120c

www.rsc.org/advances

1. Introduction

Magnetic core–shell-structured mesoporous silica microspheres are of the great interest to researchers from a wide range of disciplines, including magnetic fluids, catalysis, biotechnology/biomedicine, magnetic resonance imaging, data storage, and environmental remediation.[1,2] In addition, this class of material possesses many excellent characteristics, such as good biocompatibility, rigidity, chemical stability, high surface areas, large pore volumes, uniform and tuneable pore sizes, controllable surface functionalization, and resistance to microbial attack. All these properties make them promising candidates for catalytic applications and evoke new windows for the exploration in scientific research.

On the other hand, the direct reduction of aromatic nitro compounds to the corresponding anilines is one of the toughest challenges today for researchers and has extensive application in organic synthesis.[3] Although a variety of methods has been well documented[4–9] for this purpose, however, some of these protocols bear drawbacks such as long reaction time, use of a toxic and expensive catalyst, carcinogenic solvent, unavailability and reusability of the catalyst. Therefore, there is still need for a green catalyst which can dominate one or more drawbacks and also an environmentally benign procedure to synthesize aromatic amines.

By considering all the above-mentioned points and in continuation of our research to develop green chemistry by using water as reaction medium and molecular host–guest

---

Chemistry Department, College of Science, Shahid Chamran University, Ahvaz, 61357-4-3169, Iran. E-mail: akiasat@scu.ac.ir; Fax: +98 61 333728044; Tel: +98 61 333728044

systems,[10–12] herein, we have focused our interest on the synthesis of core–shell structured microsphere with a superparamagnetic core, a middle nonporous silica shell and an outer organo functionalized mesoporous silica shell, in order to render its suitable as a host to support silver nanoparticles. The catalytic activity of the synthesized nanocomposite, Fe_3O_4@*n*SiO_2@*m*SiO_2/Pr-Im-NH_2·Ag was investigated for the reduction of nitroarenes to the corresponding aromatic amines by using $NaBH_4$ as reducing agent in aqueous medium.

2. Experimental

2.1. General

Iron(II) chloride tetrahydrate (99%), iron(III) chloride hexahydrate (98%), cetyl trimethyl ammonium bromide (CTAB), ammonia, concentrated HCl, tetraethyl orthosilicate (TEOS), 3-chloropropyltriethoxysilane (CPTES) and nitrobenzene derivatives were purchased from Fluka and Merck companies and used without further purification. The products were characterized by comparison of their physical data, FT-IR, H & ^{13}C NMR, spectra with known samples. The purity determination of the products and reaction monitoring were accomplished by TLC on silica gel PolyGram SILG/UV 254 plates. FT-IR spectra of the powders were recorded using BOMEM MB-Series 1998 FT-IR spectrometer. The TGA curve of the nanocomposite was recorded on a BAHR SPA 503 at heating rates of 10 °C min^{-1} under air atmosphere, over the temperature range of 25–600 °C. TEM images were taken using a Zeiss-EM10C at 80 kV. X-ray diffraction (XRD) patterns of samples were taken on Philips X-ray diffraction Model PW 1840. The magnetic properties were investigated with a vibrating magnetometer (Meghnatis Daghigh Kavir Co., Kashan, Iran).

2.2. Preparation of Fe_3O_4 superparamagnetic nanoparticles

Superparamagnetic nanoparticles (MNPs) were prepared *via* improved chemical coprecipitation method.[13] According to this method, $FeCl_2·4H_2O$ (6.346 g, 31.905 mmol) and $FeCl_3·6H_2O$ (15.136 g, 55.987 mmol) were dissolved in 640 mL of deionized water. The mixed solution was stirred under N_2 at 90 °C for 1 h. 80 mL of $NH_3·H_2O$ (25%) was injected into the reaction mixture rapidly, stirred under N_2 for another 1 h and then cooled to room temperature. The precipitated particles were washed with hot water and separated by magnetic decantation. Finally, magnetic NPs were dried under vacuum at 70 °C.

2.3. Preparation of Fe_3O_4@*n*SiO_2@*m*SiO_2 microspheres

Fe_3O_4@*n*SiO_2 core–shell microspheres were prepared *via* a hydrolysis reaction. In a typical synthesis, 0.1 g of as-prepared Fe_3O_4 microspheres was firstly washed with 50 mL of HCl solution (0.1 M), and then dispersed in a solution containing 80 mL of ethanol and 20 mL of H_2O mixed with 1 mL of aqueous ammonia (25 wt%). After 15 min of ultrasonication, 0.5 mL of tetraethyl orthosilicate (TEOS) was added dropwise into the mixture and under violent stirring at room temperature the reaction continued for 24 h. The product was separated by an external magnet and washed with ethanol and deionized water for several times. The final product was collected and dried at 60 °C. The mesoporous SiO_2 shells were achieved by treating the obtained Fe_3O_4@*n*SiO_2 microspheres with a hydrothermal method. Typically, 0.1 g of the as-synthesized Fe_3O_4@*n*SiO_2 microspheres was dispersed in a mixed solution of ethanol (60 mL), deionized water (80 mL), cetyltrimethyl ammonium bromide (CTAB, 0.3 g), and 1.1 mL of aqueous ammonia (25 wt%) by ultrasonication for 15 min. Then 0.5 mL of TEOS was added into the above suspension under stirring. After reacting for 16 h at room temperature, the product was collected by magnetic separation, washed first with an ethanol/HCl (95/5, v/v) solution to remove the surfactant template, and then with ethanol and deionized water. The final product was dried at 60 °C, and denoted as Fe_3O_4@*n*SiO_2@*m*SiO_2.

2.4. Synthesis of Fe_3O_4@*n*SiO_2@*m*SiO_2-propyl-3-aminoethyl imidazolium bromide, Fe_3O_4@*n*SiO_2@*m*SiO_2@Pr-Imi-NH_2

2.4.1. Grafting of the propyl chloride unites on the surface of the Fe_3O_4@*n*SiO_2@*m*SiO_2 microspheres, synthesis of Fe_3O_4@*n*SiO_2@*m*SiO_2@Pr–Cl. To prepare Fe_3O_4@*n*SiO_2@*m*SiO_2@Pr–Cl, 0.4 mL (1.66 mmol) of CPTES was added slowly into a mixture of 0.2 g of Fe_3O_4@*n*SiO_2@*m*SiO_2 and 20 mL of dry toluene. The reaction mixture was refluxed in an oil bath. After 24 h of refluxing, the flask was cooled to room temperature. The solid phase was filtered and washed twice with dry toluene, once with ethanol and distilled water to remove the un-reacted CPTES. The nanocomposite was then dried at 100 °C for 24 h.

2.4.2. Grafting of the propyl-3-aminoethyl imidazolium bromide unites on the surface of the Fe_3O_4@*n*SiO_2@*m*SiO_2 microspheres, synthesis of Fe_3O_4@*n*SiO_2@*m*SiO_2@Pr-Imi-NH_2. To a solution of imidazole (0.136 g, 2 mmol) in 25 mL of dry toluene, sodium hydride (0.048 g, 2 mmol) was added and stirred under a nitrogen atmosphere at room temperature for 2 h to give sodium imidazole.[14] Then Fe_3O_4@*n*SiO_2@*m*SiO_2@Pr–Cl (0.3 g) was added and the mixture was refluxed under a nitrogen atmosphere for 24 h. The resulting product was filtered and washed with ethanol (3 × 20 mL) and dried under vacuum at 100 °C for 8 h to give Fe_3O_4@*n*SiO_2@*m*SiO_2@Pr-Imi. Then, to the suspension of Fe_3O_4@*n*SiO_2@*m*SiO_2@Pr-Imi (0.3 g, 2 mmol) in 25 mL of acetonitrile, 2-bromo ethyl amine hydrobromide (0.408 g, 2 mmol) was slowly added and the mixture was refluxed at 80 °C for 12 h. The excess 2-bromo ethyl amine hydrobromide was removed by filtration, followed by repeated washing with ethanol. The resulting solid was washed with NaOH (0.05 g, 1.25 mmol) for neutralization and dried in an oven at 80 °C for 6 h.

2.5. Immobilization of silver nanoparticles onto the Fe_3O_4@*n*SiO_2@*m*SiO_2@Pr-Imi-NH_2

0.3 g of Fe_3O_4@*n*SiO_2@*m*SiO_2@Pr-Imi-NH_2 was dispersed in 100 mL freshly prepared an aqueous solution of $NaBH_4$ (0.003 M) and the mixture was stirred for 1 h in an ice bath. To the suspension, an aqueous solution of $AgNO_3$ (100 mL of 0.001 M) was added drop wise with constant stirring. After 2 h, the ice bath was removed and the suspension was stirred for 3 h. Finally, the nanocomposite, Fe_3O_4@*n*SiO_2@*m*SiO_2@Pr-Imi-

NH_2·Ag, was filtered and washed with water for several times and dried at 45 °C. The nanocomposite was stored in a dark colour bottle.

2.6. Procedure for reduction of nitro compounds, catalyzed by Fe_3O_4@*n*SiO_2@*m*SiO_2@Pr-Imi-NH_2·Ag

In a 50 mL round bottom flask, nitroaromatic compound (1 mmol), $NaBH_4$ (5 mmol) and nanocomposite (0.02 g) were added and completely mixed at room temperature. Then water (5 mL) was added to the mixture and the resulting suspension was stirred at 95 °C for the time shown in Table 3. After completion of the reaction as indicated by TLC [using Et_2O/*n*-hexane as eluent: 1/5], the insoluble supported nanocatalyst was isolated with the aid of an external magnetic field and the aniline product was extracted from liquid with diethyl ether.

3. Results and discussions

The route for the preparation of the magnetic core–shell-structured mesoporous organosilica having Brønsted basic ionic liquid unites and its successful application as support for Ag nanoparticles is schematically illustrated in Scheme 1. For this gold, Fe_3O_4 nanoparticles were prepared by co-precipitation method and coated with silica through the hydrolysis of TEOS. For the preparation of mesoporous silica-encapsulated Fe_3O_4@*n*SiO_2@*m*SiO_2 nanoparticles, Fe_3O_4@*n*SiO_2 was coated with silica through the hydrolysis of TEOS in the presence of CTAB as a pore-forming agent. Further modification of the surface by grafting of 3-chloropropyl triethoxysilane, nucleophilic substitution reaction of the chloride with imidazole and then quaternization with 2-bromo ethylamine hydrobromide was produced 2-amino ethyl-3-propyl imidazolium bromide functionalized magnetic core–shell-structured mesoporous silica microspheres, Fe_3O_4@*n*SiO_2@*m*SiO_2@Pr-Imi-NH_2. Finally, the nanocomposite was used as a host to support silver NPs. In the preparation process, one very important step was to load the Ag nanoparticles on the SiO_2 surface. In this process, $NaBH_4$ was selected as the reductant to load Ag nanoparticles on the Fe_3O_4@*n*SiO_2@*m*SiO_2@Pr-Imi-NH_2 particles, because $NaBH_4$ could reduce the Ag^+ to Ag^0. As shown in Scheme 1, Fe_3O_4@*n*SiO_2@*m*SiO_2@Pr-Imi-NH_2·Ag was contained a super-paramagnetic core, a middle nonporous silica shell, and an outer Ag-functionalized mesoporous silica shell.

This organic–inorganic hybrid nanocomposite contains Brønsted basic ionic liquid unites. It is thought that this unites can enhance the hydrophobicity as well as the hydrophilicity of silica porous and therefore, it can be used as a solid–liquid phase transfer catalyst in the nitroarenes reduction by $NaBH_4$ in water. In addition, this arms can probably separate the supported silver nanoparticles and prevents their agglomeration.

The structure of the resulting hybrid nanocomposite, Fe_3O_4@*n*SiO_2@*m*SiO_2@Pr-Imi-NH_2·Ag, was comprehensively characterized by FT-IR spectroscopy, transmission electron microscopy (TEM), CHN analysis, thermogravimetric analysis

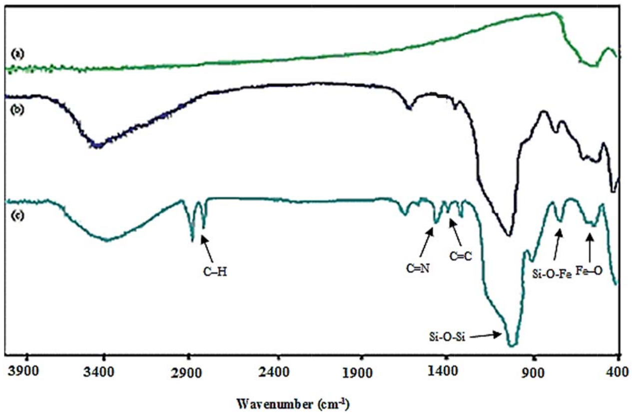

Fig. 1 The FT-IR spectra of (a) Fe_3O_4, (b) Fe_3O_4@*n*SiO_2@*m*SiO_2, (c) Fe_3O_4@*n*SiO_2@*m*SiO_2@Pr-Imi-NH_2.

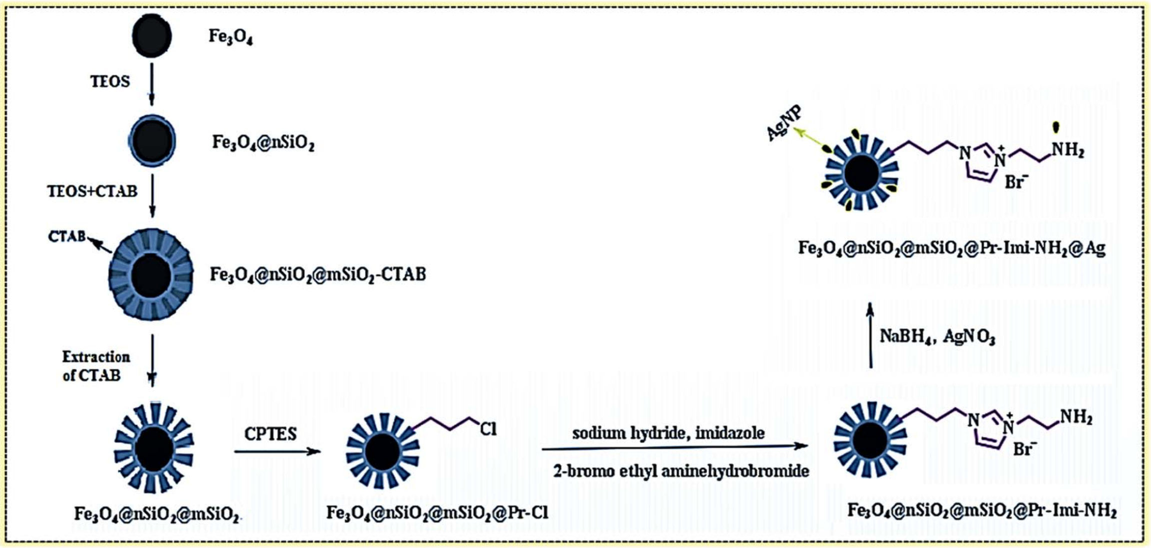

Scheme 1 Schematic illustration of the steps in the synthesis of Fe_3O_4@*n*SiO_2@*m*SiO_2/Pr-Im-NH_2·Ag.

(TGA), vibrating sample magnetometer (VAM), X-ray diffraction (XRD) and Brunauer–Emmett–Teller (BET).

Fig. 1 shows the FT-IR spectra of the Fe_3O_4 (a), Fe_3O_4@*n*SiO_2@*m*SiO_2 (b), Fe_3O_4@*n*SiO_2@*m*SiO_2@Pr-Imi-NH_2 (c) in the range of 400–4000 cm^{-1}. The characteristic band of Fe–O appeared at about 582 cm^{-1} in all spectrums. Fig. 1b indicates absorption bands at 1090, 989, 801 cm^{-1} that corresponded to the stretching vibration of Si–O–Si, Si–OH, and Si–O–Fe bonds, respectively, that indicating the SiO_2 shell was indeed coated onto the surfaces of Fe_3O_4 nanoparticles. In addition, the FT-IR spectra of the Fe_3O_4@*n*SiO_2@*m*SiO_2@Pr-Imi-NH_2 exhibited two new peaks display at 1511 and 1615 cm^{-1} which were assigned to C=C, C=N bands of the imidazole ring, respectively. The bands in the range of 2800–3000 cm^{-1} corresponded to the stretching vibration of C–H bonds of the methylene groups that indicates successful grafting of organic groups to silica in Fig. 1c.

The X-ray diffraction (XRD) pattern of Fe_3O_4@*n*SiO_2@*m*SiO_2@Pr-Imi-$NH_2 \cdot$Ag is shown in Fig. 2. It exists a broad peak at $2\theta = 22$ that indicates the coated SiO_2 shell is amorphous. The obvious diffraction peaks at 2θ values of 38.1, 44.3, 64.4, and 77.3, were corresponding to the (111), (200), (220), and (311) planes of silver (marked ○), respectively. In addition, the peaks located at $2\theta = 30.5$, 35.7, 43.29, 53.68, 57.18, and 62.79 were

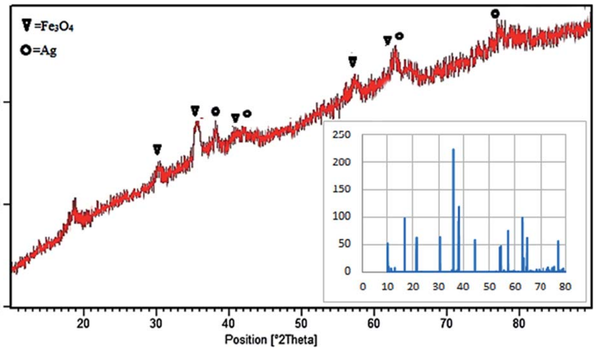

Fig. 2 The X-ray diffraction pattern for Fe_3O_4@*n*SiO_2@*m*SiO_2@Pr-Imi-$NH_2 \cdot$Ag.

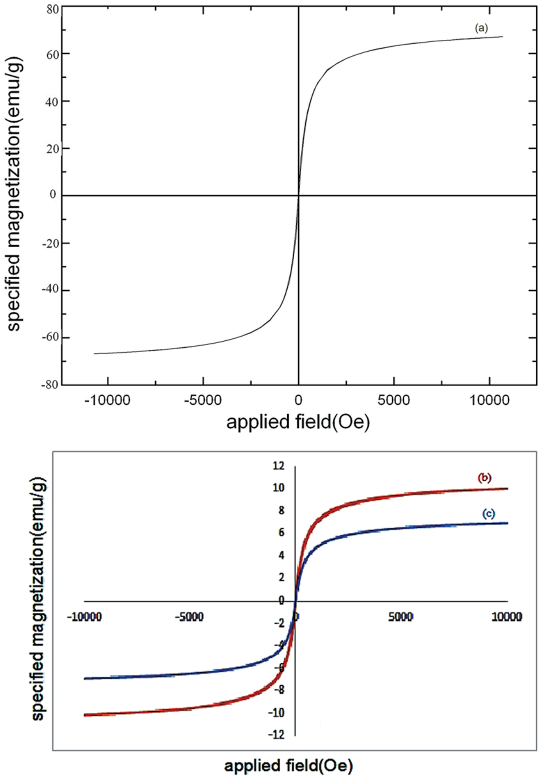

Fig. 3 VSM magnetization curves of the Fe_3O_4 (a), Fe_3O_4@*n*SiO_2@*m*SiO_2/Pr-Imi-NH_2 (b) and Fe_3O_4@*n*SiO_2@*m*SiO_2/Pr-Imi-$NH_2 \cdot$Ag (c) nanoparticles.

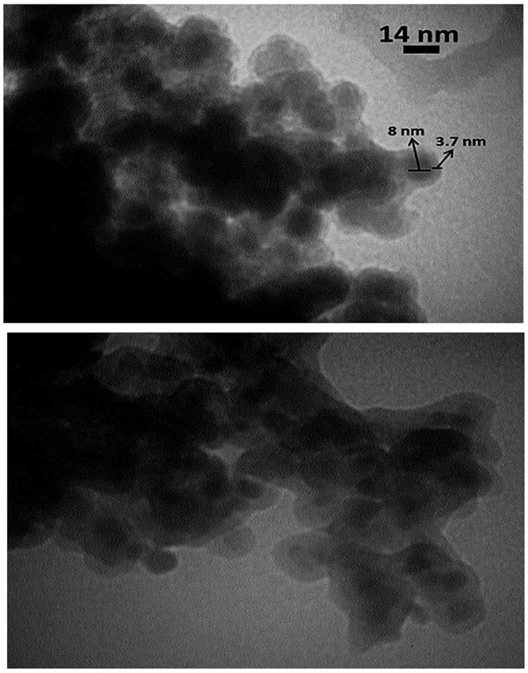

Fig. 4 TEM images of Fe_3O_4@*n*SiO_2@*m*SiO_2@Pr-Imi-$NH_2 \cdot$Ag core–shell nanostructures.

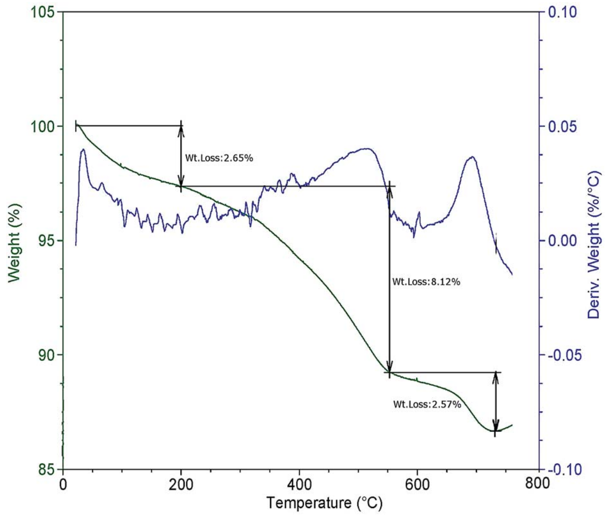

Fig. 5 TGA-DTA analysis of Fe_3O_4@*n*SiO_2@*m*SiO_2@Pr-Imi-NH_2.

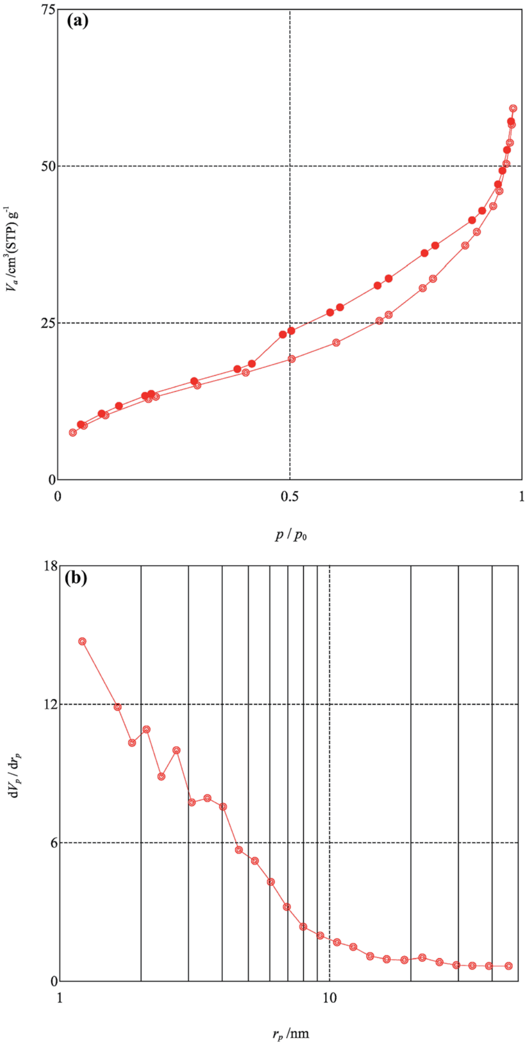

Fig. 6 Nitrogen adsorption–desorption (a) and pore size distributions (b) isotherms of Fe_3O_4@$n$$SiO_2$@$m$$SiO_2$@Pr-Imi-$NH_2$.

Table 1 Optimization of the amount of the Fe_3O_4@$n$$SiO_2$@$m$$SiO_2$/Pr-Imi-$NH_2$·Ag as catalyst for the reduction of nitrobenzene in water at 95 °C

Entry	Catalyst (g)	$NaBH_4$ (mmol)	Time (min)	Yield (%)
1	—	6	240	Trace
2	0.01	5	60	85
3	0.02	5	45	98
4	0.05	5	45	98
5	0.05	6	45	99
6	0.1	6	40	98

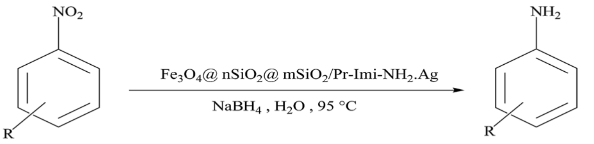

Scheme 2 Reduction of the nitroarenes.

Table 2 Reduction of nitroarenes by $NaBH_4$ in the presence of Fe_3O_4@$n$$SiO_2$@$m$$SiO_2$/Pr-Imi-$NH_2$·Ag in water ($NaBH_4$/nitro compound: 5 : 1, temperature: 95 °C)

Entry	Substrate	Product	Time (min)	Yield (%)
1	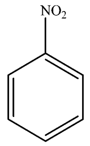	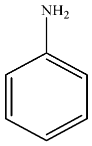	40	98
2	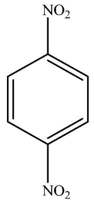	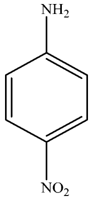	20	98
3	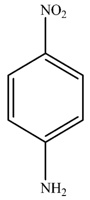	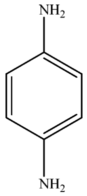	55	95
4	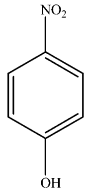	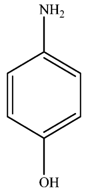	45	90
5	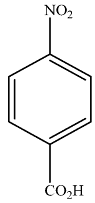	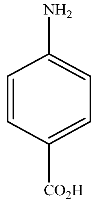	35	80
6	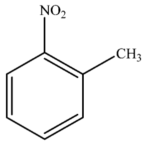	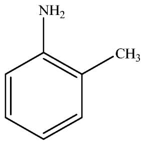	50	90
7	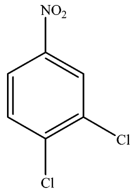	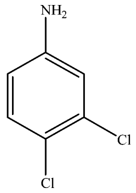	45	97
8	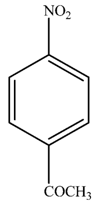	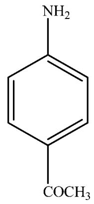	30	92

corresponding to the (220), (311), (400), (422), (511), and (440) planes of Fe_3O_4, (marked ▽), respectively.

The magnetic properties of the synthesized Fe_3O_4 and silica coated Fe_3O_4 nanoparticles were analyzed by VSM, as shown in Fig. 3. The saturated magnetization value (M_s) of the Fe_3O_4 (a), Fe_3O_4@*n*SiO_2@*m*SiO_2@Pr-Imi-NH_2 (b) and Fe_3O_4@*n*SiO_2@*m*SiO_2@Pr-Imi-$NH_2\cdot$Ag (c) were 69, 10 and 7 emu g^{-1}, respectively. The reason of observed reductions could be explained because of SiO_2 coating and supporting Ag nanoparticles on the surface of Fe_3O_4 nanoparticles.

In order to further characterize the catalyst, and to confirm the immobilization of the organic components on the pore surface, CHN analysis was utilized. The results of elemental analysis showed the presence of carbon (7.6%), nitrogen (2.5%) and hydrogen (9.8%).

In addition, the Ag content of the nanocomposite was determined by atomic absorption spectroscopy using standard addition method and confirmed by UV-vis spectroscopy (loading *ca.* 0.0556 ± 0.001 mmol g^{-1}).

The morphology and particle size distribution of Fe_3O_4@*n*SiO_2@*m*SiO_2@Pr-Imi-$NH_2\cdot$Ag nanostructure was examined by TEM. Fig. 4 reveals that Fe_3O_4@*n*SiO_2@*m*SiO_2@Pr-Imi-$NH_2\cdot$Ag has spherical shape and core–shell structured magnetic silica microspheres with nano dimension ranging under 30 nm.

TGA analysis of the nanoparticle was also used to determine the content of organic functional groups of the sample and their thermal stability. Fig. 5 showed the thermogravimetric analysis-derivative thermogravimetric analysis (TGA-DTG) for Fe_3O_4@*n*SiO_2@*m*SiO_2/Pr-Im-NH_2. The TGA curve showed that the emission mass fraction of water was about 2.65% when the temperature was less than 200 °C and the other decrease in weight was 10.70% in the temperature range from *ca.* 200 to 730 °C should be ascribed to the decomposition of groups grafted to the silica surface during hydrothermal treatment. It could easily be seen that the total content of the magnetic nucleus and silica shell in the Fe_3O_4@*n*SiO_2@*m*SiO_2/Pr-Im-NH_2 is about 86.6%. In addition, the results of TGA prove that the attachment of organic groups onto the surface of Fe_3O_4@*n*SiO_2@*m*SiO_2 nanoparticle and it can be seen from the organic groups content which is similar to the results of elemental analysis (EA). On the basis of the result of EA about 0.107 g g^{-1} of organic ligand is grafted on the carriers.

The textural property of Fe_3O_4@*n*SiO_2@*m*SiO_2/Pr-Im-NH_2 was characterized *via* nitrogen gas porosity measurements. Fig. 6 shows the N_2 adsorption–desorption isotherms and pore size distributions. The nitrogen sorption isotherms of magnetic core–shell nanocomposite exhibited typical type IV isotherm with a hysteresis loop of type H_2 at P/P_0 between 0.4 and 1.0 which is characteristic of mesoporous materials (according to the IUPAC classification), characteristics of pores with indefinite form and size, according to the TEM images. In addition, the measured BET surface area, BJH pore volume and pore size is 45.42 m^2 g^{-1}, 0.31 cm^3 g^{-1} and 8 nm, respectively. The appropriate surface area and pore volume can provide a favorable space for anchoring Ag NPs.

After characterization, the catalytic performance of this heterogeneous organocatalyst has been systematically studied in the aqueous reduction of nitroarenes by $NaBH_4$. The nitrobenzene reduction was examined as a model reaction to determine whether the use of Fe_3O_4@*n*SiO_2@*m*SiO_2@Pr-Imi-$NH_2\cdot$Ag was efficient and to investigate the optimized conditions (Table 1).

After some experiments, it was found that for facile reduction of 1 mmol of nitrobenzene, the use of 5 mmol of $NaBH_4$ in the presence of Fe_3O_4@*n*SiO_2@*m*SiO_2@Pr-Imi-$NH_2\cdot$Ag (0.02 g) at 95 °C was the best condition. In order to elucidate the role of catalyst, a control reaction was set up in the absence of a catalyst. It was found that in the absence of catalyst only trace amount of the desired product was observed on the TLC plate even after 6 h of heating.

Using the optimized reaction conditions, the activity and the scope of the catalyst was explored in the reduction of a variety of nitroarenes (Scheme 2, Table 2). As shown in Table 2, electron withdrawing/donating groups have a very small influence on the reaction times and yields. In all cases, aniline derivatives were found to be the only product of the reactions and the azoxy, azo and hydrazo compounds as the usual side products in the reduction of nitroarenes were not observed.

Noteworthy is that highly chemoselective reactions were achieved in the presence of other functional groups such as halogen, carboxylic acid, and ester groups. The silver particles immobilized on silica gel are stable in the presence of oxygen for several months.

Table 3 Comparison of the present system with the some recently reported procedures in the nitrobenzene reduction

No.	Catalytic system	Reaction conditions	Yield	Ref.
1	Polymer supported palladium nanoparticles	$NaBH_4$, H_2O, 6 h, R.T, catalyst (0.04 g)	96%	15
2	Silica gel supported PEG and zinc powder	Water, reflux, 1 h, catalyst (0.1 g)	86%	16
3	NAP–Mg–Pd(0)/PS[a]	Et_3N, PMHS, H_2O, 80 °C, 2 h, catalyst (0.02 g)	97%	17
4	Silver nanoparticles immobilized to rice husk–SiO_2–aminopropylsilane composite	$NaBH_4$, H_2O, reflux, 50 min, catalyst (0.5 g)	95%	18
5	Ag/SiO_2	EtOH, pressure to 2 MPa, 140 °C, 3 h, catalyst (0.5 g)	100%	19
6	Scrap automobile catalyst	$NaBH_4$, EtOH/water (1/1), 5 °C, 4 h, catalyst (0.3 g)	95%	20
7	(c-Pt + Mo)/C[b]	EtOH/water, H_2 (4 bar, total pressure), 30 °C, 50 min, catalyst (0.07 g)	99%	21
8	Present catalyst	$NaBH_4$, H_2O, reflux, 45 min, catalyst (0.02 g)	98%	This work

[a] Polysiloxane-stabilised "Pd" nanoparticles on NAP–magnesium oxide supports. [b] Pt NPs supported on activated carbon and promoted by a molybdenum salt.

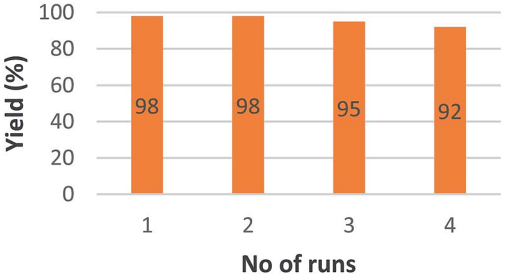

Fig. 7 Recyclability of $Fe_3O_4@nSiO_2@mSiO_2$/Pr-Imi-$NH_2\cdot$Ag in the nitrobenzene reduction in water after 40 min.

The catalytic efficiency of the $Fe_3O_4@nSiO_2@mSiO_2$@Pr-Imi-$NH_2\cdot$Ag nanocatalyst was compared with that of a number of previously reported catalysts in the reduction of nitroarenes reaction (Table 3). The results demonstrate that, although, the former catalytic systems have a reasonably high activity for conversion of a set of various nitroarenes to their corresponding aniline derivatives, but the reactions were performed with a large amount of catalyst and in longer times than with the present catalyst.

The reusability of the catalyst was also tested. For this gold, after completion of the reduction of nitrobenzene, the $Fe_3O_4@nSiO_2@mSiO_2$@Pr-Imi-$NH_2\cdot$Ag was easily separated from the reaction mixture by means of an external magnetic field and washed with water and diethyl ether and then dried and reused for four times under one constant set of operating conditions ($NaBH_4$/nitrobenzene: 5 : 1, temperature: 95 °C, time: 40 min). As shown in Fig. 7, the average chemical yield for four consecutive runs was 95.7% after 40 min which clearly demonstrates the practical recyclability of this catalyst.

4. Conclusion

In this study, we report a successful synthesis of core–shell nanoparticles with a superparamagnetic iron oxide core, a middle nonporous silica shell and an outer organo functionalized mesoporous silica shell, and evaluated for immobilizing of Ag nanoparticles. The resulting $Fe_3O_4@nSiO_2@mSiO_2$@Pr-Imi-$NH_2\cdot$Ag core–shell microsphere was utilized as a recyclable catalyst in an aqueous medium for the reduction of nitroarenes to the corresponding amines by using $NaBH_4$ as reducing agent. The nanocatalyst can be easily isolated from the reaction mixture by using a magnetic field and directly used in the next reaction cycles without a significant loss of its activity. This novel methodology was also enhanced product purity and promises economic as well as environmental benefits.

Acknowledgements

We gratefully acknowledge the support of this work by Shahid Chamran University Research Council.

Notes and references

1 Y. Long, M. Xie, J. Niu, P. Wang and J. Ma, *Appl. Surf. Sci.*, 2013, **277**, 288.
2 L. Zhao, Y. Chi, Q. Yuan, N. Li, W. Yan and X. Li, *J. Colloid Interface Sci.*, 2013, **390**, 70.
3 H. K. Kadam and S. G. Tilve, *RSC Adv.*, 2012, **2**, 6057.
4 C. Yang and C. U. Pittman, *Synth. Commun.*, 1998, **28**, 2027.
5 A. S. Kende and J. S. Mendoza, *Tetrahedron Lett.*, 1991, **32**, 1699.
6 K. P. Chary, S. R. Ram and D. S. Iyengar, *Synlett*, 2000, **5**, 683.
7 M. Kumarraja and K. Pitchumani, *Appl. Catal., A*, 2004, **265**, 135.
8 D. Gaofei, S. Yan, F. Zhifeng and Y. Wantai, *Chin. J. Catal.*, 2012, **33**, 651.
9 S. K. Ghosh, M. Mandal, S. Kundu, S. Nath and T. Pal, *Appl. Catal., A*, 2004, **268**, 61.
10 A. R. Kiasat and M. Fallah-Mehrjardi, *Catal. Commun.*, 2008, **9**, 1497.
11 A. R. Kiasat, R. Badri, B. Zargar and S. Sayyahi, *J. Org. Chem.*, 2008, **73**, 8382.
12 A. R. Kiasat and S. Nazari, *Catal. Sci. Technol.*, 2012, **2**, 1056.
13 K. D. Kim, S. S. Kim, Y. H. Choa and H. T. Kim, *J. Ind. Eng. Chem.*, 2007, **13**, 1137.
14 A. S. Amarasekara and O. S. Owereh, *Catal. Commun.*, 2010, **11**, 1072.
15 M. M. Dell'Anna, S. Intini and G. Romanazzi, *J. Mol. Catal. A: Chem.*, 2014, **395**, 307.
16 A. R. Kiasat, M. Zayadi and F. Mohammad-Taheri, *Iran. J. Chem. Chem. Eng.*, 2011, **2**, 30.
17 D. Damodara, R. Arundhathi, T. V. Ramesh Babu, M. K. Legan, H. J. Kumpaty and P. R. Likhar, *RSC Adv.*, 2014, **4**, 22567.
18 J. Davarpanah and A. R. Kiasat, *Catal. Commun.*, 2013, **41**, 6.
19 Y. Chen, C. Wang, H. Liu, J. Qiu and X. Bao, *Chem. Commun.*, 2005, **42**, 5298.
20 H. Genc, *Catal. Commun.*, 2015, **67**, 64.
21 E. Boymans, S. Boland, P. T. Witte, C. Muller and D. Vogt, *ChemCatChem*, 2013, **5**, 431.